

ICE SHEETS

Friction at the bed does not control fast glacier flow

L. A. Stearns^{1,2*} and C. J. van der Veen³

The largest uncertainty in the ice sheet models used to predict future sea level rise originates from our limited understanding of processes at the ice/bed interface. Near glacier termini, where basal sliding controls ice flow, most predictive ice sheet models use a parameterization of sliding that has been theoretically derived for glacier flow over a hard bed. We find that this sliding relation does not apply to the 140 Greenland glaciers that we analyzed. There is no relationship between basal sliding and frictional stress at the glacier bed, contrary to theoretical predictions. There is a strong relationship between sliding speed and net pressure at the glacier bed. This latter finding is in agreement with earlier observations of mountain glaciers that have been largely overlooked by the glaciological community.

The Greenland Ice Sheet (GrIS) has lost mass at an accelerated rate over the past two decades (1, 2), a conclusion that the Intergovernmental Panel on Climate Change's Fifth Assessment Report states with "high confidence" (3). However, projections for future mass loss are at a "fairly early stage" (3), particularly regarding predictions of outlet glacier behavior (4–7). In Greenland, drainage of interior ice is accomplished through some 242 outlet glaciers (8), the majority of which move at speeds that cannot be achieved by internal deformation alone, indicating that basal sliding is an important contributor to ice discharge and mass loss to the oceans. Parameterizing how ice flows over its bed (the "sliding relation"), and how this flow varies over space and time and in a changing climate, remains a long-held goal for ice sheet modelers.

Processes operating at the ice/bed interface involve interactions among ice, water, and geological solids (9). The complexity of these processes may preclude the formulation of a simple model or law describing how the basal ice velocity is related to properties such as basal drag, water pressure and water quantity beneath the glacier, sediment viscosity, and a number of other factors. Nevertheless, it is important to evaluate whether any proposed sliding relation actually applies to real ice sheets. This is of particular relevance because recent studies suggest that the behavior and sensitivity of marine-terminating outlet glaciers may depend critically on the prescribed sliding law (10).

Most ice sheet models rely on a sliding relation that relates the sliding velocity to frictional stress

(the modified Weertman model) (11), applicable when the interface is a hard bed

$$U_s = A_s \frac{\tau_b^p}{N_e^q} \quad (1)$$

where U_s represents the sliding velocity, τ_b is friction at the ice/bed interface, N_e is the effective pressure at the glacier bed (the difference between the weight of the ice and water pressure at the bed), and p and q are unknown exponents assumed to be constant over the ice sheet. The sliding parameter, A_s , is often assumed to be a function of available meltwater to simulate seasonal speed-up events (7), whereas the effective pressure is often equated with the height above buoyancy (7)

$$H_{ab} = H - \frac{\rho_w}{\rho_i} D \quad (2)$$

Here, H is the ice thickness, D is the water depth, and ρ_w and ρ_i are the density of seawater and ice, respectively. Taking the natural logarithm of Eq. 1 allows the effects of basal drag and effective pressure on the sliding velocity to be investigated separately, that is

$$\ln(U_s) = \ln(A_s) + p \ln(\tau_b) - q \ln(N_e) \quad (3)$$

In this study, we explore the sliding relation (Eq. 3) using measurements of ice velocity and estimates of basal drag for the trunks of 140 outlet glaciers that move at speeds exceeding 50 m/year (the locations of these glaciers are shown in Fig. 1, and their coordinates are listed in table S1). We selected this velocity threshold to ensure that basal sliding is the dominant mode of ice discharge. We estimated basal drag using the force-budget technique (12, 13), which calculates depth-averaged resistive stresses from measured surface strain rates; comparison with the

driving stress then yields the basal drag from the requirement that the net force acting on a section of the glacier must be zero. The assumption that surface values of strain rates can be used to estimate strain rates at depth may introduce some error in the estimated basal drag, although this error is believed to be small in regions of fast sliding (13). The main advantage of using the force-budget technique is that results do not require a sliding relation to be prescribed. This is in contrast to the control-methods approach (14–16), which finds a solution that best represents observed velocities given a relation between basal drag and basal velocity.

Our results show that the relationship between basal drag and sliding velocity does not follow Weertman-style behavior; there is no obvious relation between the natural logarithm of sliding velocity and that of basal drag. This is illustrated in Fig. 2A for the three big glaciers that account for about 40% of the discharge from the GrIS. The slope of the regression line (p in Eq. 3) is not significantly different from zero (as determined from the standard t test). Similar patterns are evident for the remaining 137 glaciers (fig. S1, table S1, and data S1).

Next, we assessed the relationship between effective pressure N_e and sliding velocity. Assuming that near the terminus, subglacial water has an easy connection to the ocean, we substituted effective pressure with height above buoyancy (7), calculated from ice geometry and water depth (17) (Eq. 2). Sliding velocity increases as the glacier approaches flotation (low height above buoyancy) (Fig. 2B). We can calculate the exponent (q ; Eq. 1) as the slope of the line in log-log space. (Here the slope is negative because N_e appears in the denominator.) In some cases, a second-order polynomial yields a somewhat better fit to the data (as determined from the coefficient of determination, R^2), especially close to the grounding line where effective pressure approaches zero. However, implementing a higher-order exponent in the sliding relation may not be numerically feasible. We find that the best linear fit for each glacier varies slightly (shown for Jakobshavn Isbræ, Kangerdlugssuaq Glacier, and Helheim Glacier in Fig. 2B), but for 90% of the 140 Greenland glaciers that we studied, the slope falls between -1.0 and -0.1 , with a mean around -0.5 (Fig. 3). Results of t tests show that the derived slopes are significant (fig. S2 and table S1).

Given the complexity of processes acting at the bed of a glacier, it is not surprising that we calculated a small range in the exponent used to relate height above buoyancy (effective pressure) to basal sliding. However, without fully understanding the physics underlying basal sliding, it is impractical to assign a unique exponent to each outlet glacier in an ice sheet model. In first approximation, the value $q = 0.5$ can be applied to all glaciers.

Our finding that height above buoyancy can be used to approximate the sliding parameter is in agreement with earlier studies of mountain glaciers. In particular, a simple inverse relation

¹Department of Geology, University of Kansas, Lawrence, KS 66045, USA. ²Center for Remote Sensing of Ice Sheets, University of Kansas, Lawrence, KS 66045, USA. ³University of Kansas, Department of Geography and Atmospheric Science, Lawrence, KS 66045, USA.

*Corresponding author. Email: stearns@ku.edu

between effective pressure and sliding speed, $U_s = A_s N_e^{-q}$, was found with $q = 0.61$ for Findelengletscher (Switzerland) and $q = 0.49$ for Storglaciären (Sweden) (18). Similar values of the exponent for mountain glaciers and ice sheet outlet glaciers imply that the processes responsible for sliding variations are also similar (18).

By adopting a sliding relation with the ice speed inversely proportional to height above buoyancy only, we can investigate the spatial pattern in the sliding parameter (Fig. 4). Our results show that the sliding parameter for individual glaciers remains relatively constant (Fig. 4D). The magnitude differences in A_s for individual glaciers represent differences in sliding speed. Obtaining a fairly constant sliding parameter along the fast-moving, lower trunk of glaciers suggests that this simplified sliding relation can appropriately reproduce spatial patterns of ice velocity. This is in stark contrast

to current modeling techniques, which involve tuning the sliding parameter to match observed velocities.

In ice sheet models, the sliding parameter needs to be tuned to reproduce both spatial and temporal variability in ice velocity. Our results show that a modified sliding relation can capture both the large-scale spatial (Fig. 4) and temporal (Fig. 5) changes in ice velocity. However, because effective pressure at the glacier base is estimated from height above buoyancy, this approximation cannot explain short-term (e.g., seasonal) variations in sliding velocity. Over short time scales, changes in surface elevation, and thus in height above buoyancy, are too small to produce the large observed velocity changes. This relationship is illustrated by the circles and triangles in Fig. 5, which correspond to seasonal changes on Helheim Glacier (19) (black markers are 15 km up-glacier; red markers are near the terminus). Circles represent winter values, and

triangles represent summer values, assuming the effective basal pressure can be estimated from the height above buoyancy. For the up-glacier location, no change in height above buoyancy is observed (19), and summer acceleration can only be explained by an increase in sliding parameter. For the terminus site, a small decrease in height above buoyancy is observed as a result of thinning (19), but to explain the seasonal acceleration, the sliding parameter must also increase. Inferred changes in A_s may be realistic, but another possibility, and perhaps more likely, is that the height above buoyancy does not accurately describe seasonal water pressure variations in the subglacial drainage system.

Seasonal (and shorter) velocity variations are related to changes in subglacial water pressure, as has been observed or inferred on many mountain glaciers (20–22). However, measurements of subglacial water pressure are rare. Direct observations in the ablation zone of the GRIS demonstrate the importance of spatiotemporal variability in water pressure in the subglacial drainage system (23). Similarly, observations of Tasman Glacier in New Zealand show that velocity variations are linked to rain-induced variations in subglacial water pressure (24). However, a simple relation between sliding speed and subglacial water pressure may not exist because expansion and contraction of subglacial cavities is driven by fluctuations in water pressure, rather than by water pressure itself (21, 22). This conclusion is in agreement with observations of the Lauteraargletscher in Switzerland (25), which show that sliding velocity is high when the water pressure is high, but the largest sliding velocities are attained when the water pressure is increasing. Our approximation of the sliding relation using height above buoyancy does not account for these important short-term variations in ice velocity but can explain larger-scale spatial and temporal patterns.

We show that the common form of the sliding relation (Eq. 1), as used in many prognostic numerical ice sheet models, does not apply to Greenland glaciers; the effect of basal drag on sliding velocity is virtually nonexistent. However, Eq. 1 was derived theoretically for the case of ice sliding over a hard bed, and there is ample evidence that Greenland glaciers largely flow over soft beds (26–30). Relations that have been proposed for deforming beds also maintain the dependency of sliding velocity on basal drag to some power (31–34), based on viscous deformation of sediment overlain by relatively clean ice. Till is assumed to deform like a plastic material, supporting shear stresses up to a yield stress, given by the Mohr-Coulomb model for saturated till. Such models have been implemented in numerical flowline models for Antarctic ice streams (35, 36), where Mohr-Coulomb relations seem to apply (31). For example, basal drag on Whillans Ice Stream in West Antarctica is less than 5 kPa, indicating that the bed is unable to support any substantive shear stress. Our calculations do not support the existence of such an upper limit on

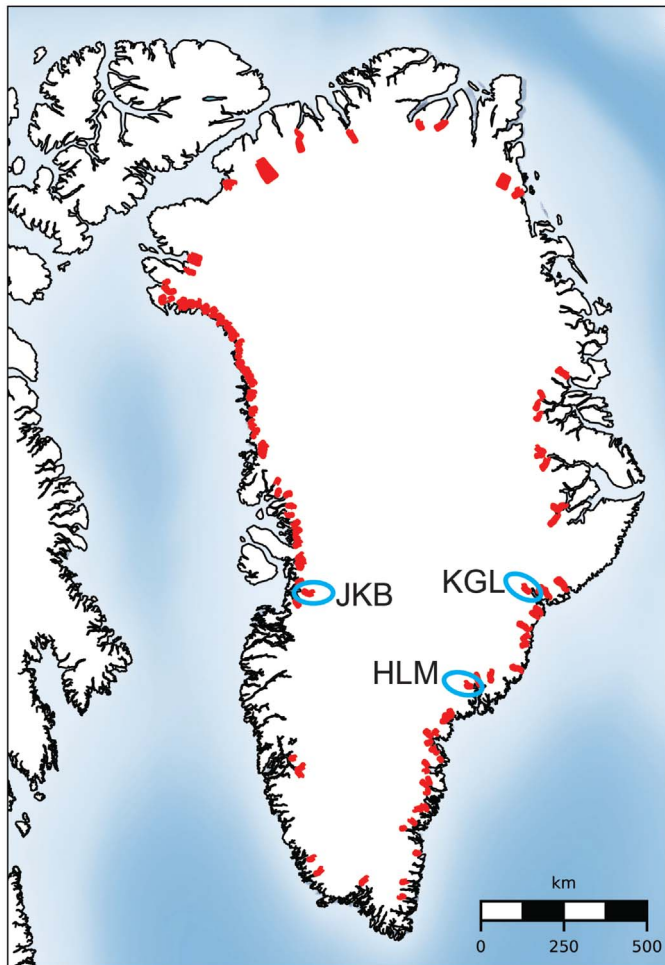


Fig. 1. Glaciers included in this study. Red polygons show the 140 marine-terminating glaciers that we analyzed. We used data extending from the grounding line up-flow to where seasonal velocity variability is <10%—on average, 15 km in length (supplementary materials). Jakobshavn Isbræ (JKB), Kangerdlugssuaq Glacier (KGL), and Helheim Glacier (HLM) are circled in blue.

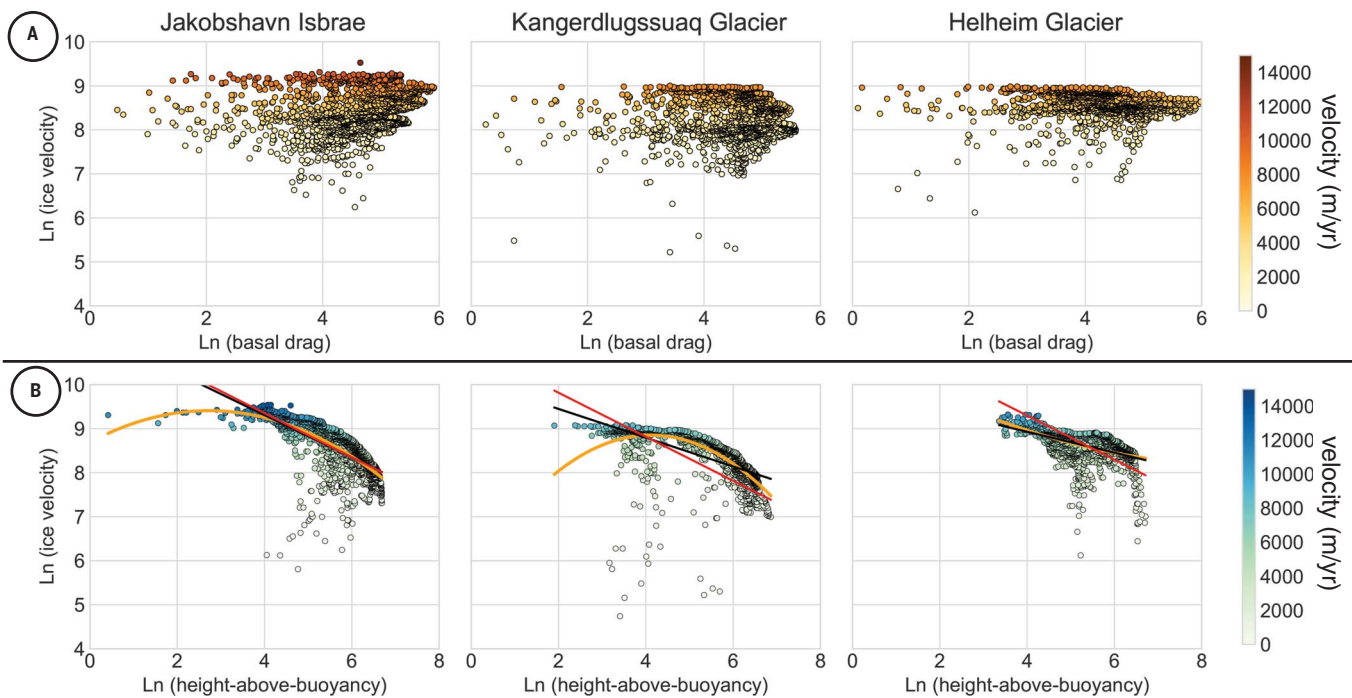


Fig. 2. Relationship between ice velocity, basal drag, and height above buoyancy. (A) Ice velocity and basal drag for the trunks of three large outlet glaciers. The uncertainty in ice velocity is 3 m/year and in basal drag is 60 kPa. (B) Ice velocity and height above buoyancy for the trunks of the same glaciers as in (A). The

uncertainty in height above buoyancy is 20 m. The best-fit line is shown in black, a linear fit with a slope of -0.5 is shown in red, and a second-order polynomial fit is shown in orange. In (A) and (B), points represent natural logarithm values and are colored by ice velocity in meters per year.

basal drag for Greenland glaciers (τ_b varies from 0 to 400 kPa). Our results, therefore, are not compatible with the proposed sliding relations based on deforming sediments beneath Greenland glaciers.

Many studies highlight the complexity of bed deformation, especially where basal ice can infiltrate the soft bed, forming a layer of ice-infiltrated till (37). Regelation infiltration observed under Engabreen, Norway, implies that increases in basal motion of the ice need not be accompanied by increases in basal drag, but rather may result from small changes in water-layer thickness (37). On Hofsjökull Ice Cap in central Iceland, which is also underlain by soft sediments, the basal shear stress is independent of basal slip rate, and observed surface speed increases in areas of faster slip (38). Glaciers in Greenland appear to behave similarly to these alpine glaciers. We posit that soft sediments effectively cover basal irregularities, reducing the bed roughness to (near) zero.

Numerical ice sheet models introduce a tunable sliding parameter to obtain agreement between modeled and observed velocities. Our results show that there is a strong relationship between height above buoyancy (effective pressure) and ice velocity; a tunable parameter is only needed to invoke short-term (seasonal) variations in sliding velocity, therefore only encompassing one main process (subglacial water pressure). In contrast, the original sliding parameter en-

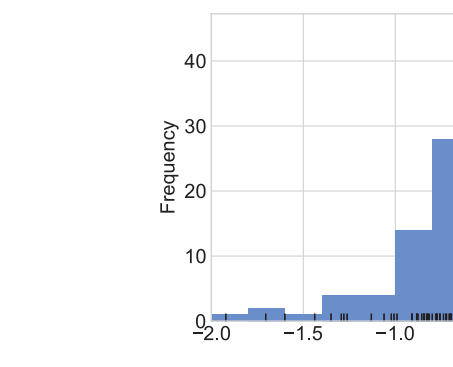


Fig. 3. Range of q values for Greenland glaciers. Best-fit slopes for $\ln(\text{ice velocity})$ versus $\ln(\text{height above buoyancy})$ for the 140 glaciers analyzed in this study. (Black tick marks represent the slopes calculated for each glacier.)

compasses a range of different processes that affect both basal friction (e.g., bed roughness, till strength, and impurities in the ice) and subglacial water pressure and needs to be tuned to both large-scale patterns and short-term variations in time and space.

The full implications for model behavior of replacing the commonly used sliding relation (Eq. 1) with an equation of the form $U_s = A_s N_e^{-q}$ are not evident. Similarly to Weertman sliding relations, this new relation does not apply at the grounding line, where effective pressure reaches

zero (and consequently the sliding velocity becomes infinite). In this region, longitudinal stress gradients need to be invoked to achieve a smooth transition in ice speed. However, our findings suggest that Greenland glaciers flow over soft sediments where small variations in basal water pressure elicit immediate changes in basal slip. Basal roughness, or features that influence basal friction, do not influence sliding speed. It is imperative for the ice sheet modeling community to explore the impact that this new relation may have on predictions of sea level rise.

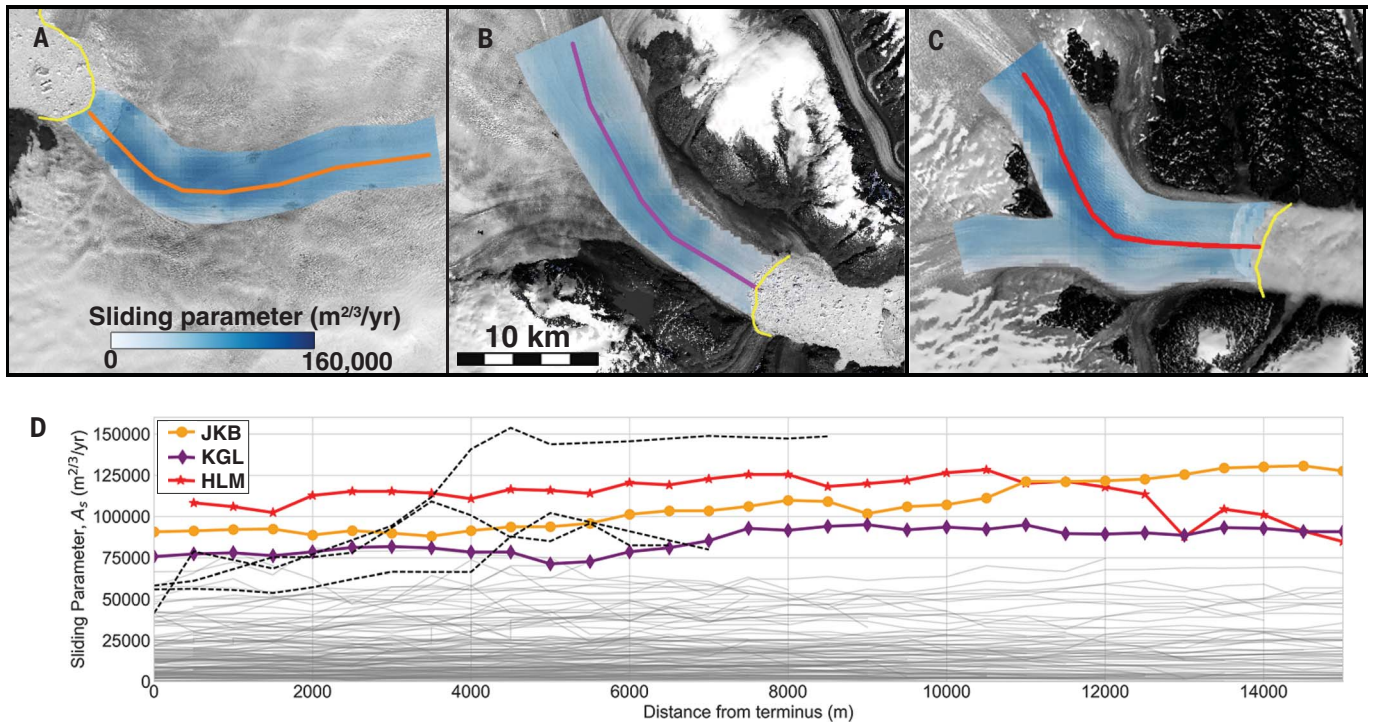


Fig. 4. Spatial distribution of the sliding parameter (A_s). Map-plane distribution of the sliding parameter over (A) Jakobshavn Isbræ, (B) Kangerdlugssuaq Glacier, and (C) Helheim Glacier. The sliding parameter is only shown over regions where basal sliding dominates and is calculated using ice thickness and ice velocity data for 2014 (supplementary materials). Center flowlines are indicated in colors corresponding to (D),

and the 2014 terminus is shown in yellow; the scale is the same for all three panels. (D) Sliding parameter values along the center flowline of all 140 glaciers in the study region. There are only three glaciers (numbers 23, 117, and 123; locations are given in fig. S1 and table S1) that show along-flow variability (black dashed lines). Uncertainty in the sliding parameter is less than 2000 m^{2/3}/year.

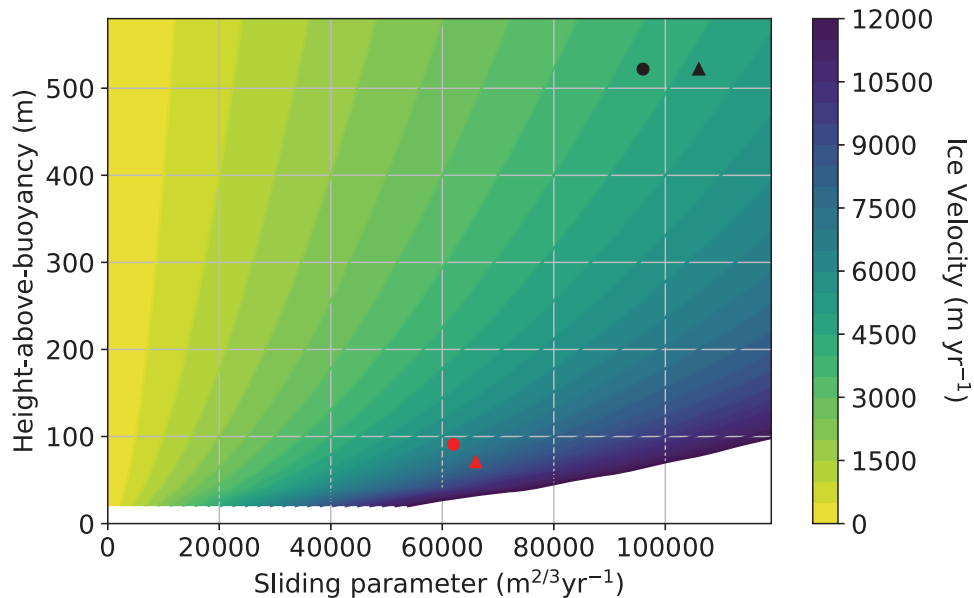


Fig. 5. The relationship between the sliding parameter, height above buoyancy, and ice velocity. Using $q = 0.5$, the sliding velocity will vary as a function of the sliding parameter and height above buoyancy (or effective pressure). Illustrated in this diagram is the observed seasonal variability (18) on Helheim Glacier near the terminus (red markers)

and 15 km up-flow of the terminus (black markers). The triangles represent summer values, and the circles represent winter values. Where height above buoyancy is small (near the terminus), small changes in sliding parameter and height above buoyancy lead to large velocity variations.

REFERENCES AND NOTES

1. M. van den Broeke *et al.*, *Science* **326**, 984–986 (2009).
2. E. M. Enderlin *et al.*, *Geophys. Res. Lett.* **41**, 866–872 (2014).
3. D. G. Vaughan, J. C. Comiso, I. Allison, J. Carrasco, G. Kaser, R. Kwok, P. Mote, T. Murray, F. Paul, J. Ren, E. Rignot, O. Solomina, K. Steffen, T. Zhang, in *Climate Change 2013: The Physical Science Basis. Contribution of Working Group I to the Fifth Assessment Report of the Intergovernmental Panel on Climate Change*, T. F. Stocker, D. Qin, G.-K. Plattner, M. Tignor, S. K. Allen, J. Boschung, A. Nauels, Y. Xia, V. Bex, P. M. Midgley, Eds. (Cambridge Univ. Press, 2013), pp. 317–382.
4. W. T. Pfeffer, J. T. Harper, S. O'Neel, *Science* **321**, 1340–1343 (2008).
5. S. F. Price, A. J. Payne, I. M. Howat, B. E. Smith, *Proc. Natl. Acad. Sci. U.S.A.* **108**, 8978–8983 (2011).
6. H. Goelzer *et al.*, *J. Glaciol.* **59**, 733–749 (2013).
7. F. M. Nick *et al.*, *Nature* **497**, 235–238 (2013).
8. E. Rignot, J. Mouginot, *Geophys. Res. Lett.* **39**, L11501 (2012).
9. G. Clarke, *Annu. Rev. Earth Planet. Sci.* **33**, 247–276 (2005).
10. J. Brondex, O. Gagliardini, F. Gillet-Chaulet, G. Durand, *J. Glaciol.* **63**, 854–866 (2017).
11. J. Weertman, *Rev. Geophys. Space Phys.* **10**, 287–333 (1972).
12. C. J. van der Veen, *Fundamentals of Glacier Dynamics*, (CRC Press, 2013).
13. I. M. Whillans, Y. H. Chen, C. J. van der Veen, T. J. Hughes, *J. Glaciol.* **35**, 68–80 (1989).
14. D. R. MacAyeal, *J. Geophys. Res. Solid Earth* **97**, 595–603 (1992).
15. E. Larour *et al.*, *J. Geophys. Res. Earth Surf.* **117**, F02009 (2012).
16. D. R. Shapero, I. Joughin, K. Poinar, M. Morlighem, F. Gillet-Chaulet, *J. Geophys. Res. Earth Surf.* **121**, 168–180 (2016).
17. M. Morlighem *et al.*, *Geophys. Res. Lett.* **44**, 11051–11061 (2017).
18. P. Jansson, *J. Glaciol.* **41**, 232–240 (1995).
19. L. Kehrl, I. Joughin, D. Shean, D. Floricioiu, L. Krieger, *J. Geophys. Res. Earth Surf.* **122**, 1635–1652 (2017).
20. A. Iken, R. A. Bindschadler, *J. Glaciol.* **32**, 101–119 (1986).
21. R. S. Anderson *et al.*, *J. Geophys. Res. Earth Surf.* **109**, F03005 (2004).
22. T. Cowton, P. Nienow, A. Sole, I. Bartholomew, D. Mair, *J. Glaciol.* **62**, 451–466 (2016).
23. L. C. Andrews *et al.*, *Nature* **514**, 80–83 (2014).
24. H. J. Horgan *et al.*, *Earth Planet. Sci. Lett.* **432**, 273–282 (2015).
25. S. Sugiyama, H. Gudmundsson, *J. Glaciol.* **50**, 353–362 (2004).
26. J. Andrews, J. D. Milliman, A. Jennings, N. Rynes, J. Dwyer, *J. Geol.* **102**, 669–683 (1994).
27. T. S. Clarke, K. Echelmeyer, *J. Glaciol.* **42**, 219–232 (1996).
28. A. D. Booth *et al.*, *Cryosphere* **6**, 909–922 (2012).
29. C. F. Dow *et al.*, *Ann. Glaciol.* **54**, 135–141 (2013).
30. F. Walter, J. Chaput, M. P. Lüthi, *Geology* **42**, 487–490 (2014).
31. R. B. Alley, D. D. Blankenship, S. Rooney, C. R. Bentley, *J. Geophys. Res. Solid Earth* **92**, 8931–8940 (1987).
32. G. Boulton, R. Hindmarsh, *J. Geophys. Res. Solid Earth* **92**, 9059–9082 (1987).
33. D. R. MacAyeal, *J. Geophys. Res. Solid Earth* **94**, 4071–4087 (1989).
34. B. Kamb, *J. Geophys. Res. Solid Earth* **96**, 16585–16595 (1991).
35. C. Schoof, *J. Fluid Mech.* **556**, 227–251 (2006).
36. E. Bueler, J. Brown, *J. Geophys. Res. Earth Surf.* **114**, F03008 (2009).
37. N. R. Iverson *et al.*, *J. Glaciol.* **53**, 323–340 (2007).
38. B. Minchew *et al.*, *J. Glaciol.* **62**, 147–158 (2016).

ACKNOWLEDGMENTS

We thank the National Snow and Ice Data Center and corresponding authors for making their data publicly available and well documented. **Funding:** This work was supported by NSF PLR 1543530 (C.J.v.d.V.) and NASA NNX11AR23G (L.A.S.).

Author contributions: L.A.S. and C.J.v.d.V. conceptualized the project, developed the methodology, and wrote the paper; L.A.S. conducted the formal analysis. **Competing interests:** The authors declare no competing interests. **Data and materials availability:** All data used in this paper are publicly available on the NSIDC website (bed topography, NSIDC-1DBMG4; ice velocity, NSIDC-0481; surface elevation, NSIDC-0715). Derived products—sliding parameter, basal drag, and height above buoyancy—are available in the supplementary materials (data S1 to S3).

SUPPLEMENTARY MATERIALS

www.sciencemag.org/content/361/6399/273/suppl/DC1
Materials and Methods
Figs. S1 to S3
Table S1
References (39–46)
Data S1 to S3

19 February 2018; accepted 24 May 2018
Published online 7 June 2018
10.1126/science.aat2217

Friction at the bed does not control fast glacier flow

L. A. Stearns and C. J. van der Veen

Science **361** (6399), 273-277.

DOI: 10.1126/science.aat2217 originally published online June 7, 2018

Sliding at the base

Predictions of sea level rise caused by dynamic ice sheet loss rely on a good understanding of what controls how fast the sheets slide over the ground below. The standard approach is to model motion on the basis of an assumed frictional stress between the base of the glacier and a hard underlying bed. Now, however, Stearns and van der Veen show that this method is incorrect. Instead, they suggest that net pressure at the glacier bed controls flow.

Science, this issue p. 273

ARTICLE TOOLS

<http://science.sciencemag.org/content/361/6399/273>

SUPPLEMENTARY MATERIALS

<http://science.sciencemag.org/content/suppl/2018/06/06/science.aat2217.DC1>

RELATED CONTENT

<http://science.sciencemag.org/content/sci/363/6427/eaau6055.full>
<http://science.sciencemag.org/content/sci/363/6427/eaau8375.full>

REFERENCES

This article cites 39 articles, 4 of which you can access for free
<http://science.sciencemag.org/content/361/6399/273#BIBL>

PERMISSIONS

<http://www.sciencemag.org/help/reprints-and-permissions>

Use of this article is subject to the [Terms of Service](#)

Science (print ISSN 0036-8075; online ISSN 1095-9203) is published by the American Association for the Advancement of Science, 1200 New York Avenue NW, Washington, DC 20005. The title *Science* is a registered trademark of AAAS.

Copyright © 2018 The Authors, some rights reserved; exclusive licensee American Association for the Advancement of Science. No claim to original U.S. Government Works